4-15-2005

Modeling, Fabrication, and Optimization of Niobium Cavities: Phase III Fourth Quarterly Report

Robert A. Schill Jr.
University of Nevada, Las Vegas, robert.schill@unlv.edu

Mohamed Trabia
University of Nevada, Las Vegas, mbt@me.unlv.edu

William Culbreth
University of Nevada, Las Vegas, william.culbreth@unlv.edu

Modeling, Fabrication, and Optimization of Niobium Cavities –Phase III
Fourth Quarterly Report – No Cost Extension Period

Principal Investigators (PI): Robert A. Schill, Jr.
Department of Electrical & Computer Engineering, UNLV
4505 Maryland Parkway, Las Vegas, NV 89154-4026
Phone: (702) 895-1526
Email: schill@ee.unlv.edu

Mohamed B. Trabia
Department of Mechanical Engineering, UNLV
4505 Maryland Parkway, Las Vegas, NV 89154-4027
Phone: (702) 895-0957
Email: mbt@me.unlv.edu

Investigator: William Culbreth
Department of Mechanical Engineering, UNLV
4505 Maryland Parkway, Las Vegas, NV 89154-4027
Phone: (702) 895-3426
Email: culbreti@nscee.edu

Current Students: Anoop George (Graduate Student)

Collaborators (DOE): Dr. Tsuyoshi Tajima, Team Leader
Accelerator Physics & Engineering
LANSCE-1
Los Alamos National Laboratory
MS H817
Los Alamos, NM 87545
Phone: (505) 667-6559
Email: tajima@lanl.gov

AAA Research Area: Accelerators / Transmuter

Abstract

Niobium cavities are important parts of the integrated NC/SC high-power linacs. Over the years, researchers in several countries have tested various cavity shapes. They concluded that elliptically shaped cells are the most appropriate shape for niobium superconducting cavities. The surface preparation can significantly affect the secondary electron emission yields. Such yields are used in design codes. Current codes use values obtained from niobium samples cleaned by a different means at temperatures other than the operating temperature. Secondary electron emission studies on LANL surface-cleaned niobium are conducted with preliminary data presented in this report at room temperature. Soon studies will be performed on surfaced cleaned samples near cryogenic temperatures.

Code Development

The Monte Carlo Back Scattering and Secondary Electron Scattering code developed by Dr. David Joy (ORNL and University of Tennessee Knoxville) has been placed on a C++ format offering fast computational speed. The architecture of the code has been modified to track multiple generations of secondary electrons. The original code only followed the secondary electrons generated by the primary electron. The model is based on Dr. David Joy's experience in the secondary electron microscopy. The code has been modified to take into consideration four or more layers which can represent a surface contaminant. A more rigorous treatment of the elastic and inelastic process of multiple components in each layer has been carefully incorporated in the code. The current version of the code does not have a graphical user interface illustrating the particle dynamics as in the original code. As a result, a visual of the code outputs is not presented here.

Experimental Study of SEE from Niobium

Near the end of the August 2004 of phase III, the main components of the secondary electron emission test stand have been assembled. Figures 1a and 1b illustrate the test stand.

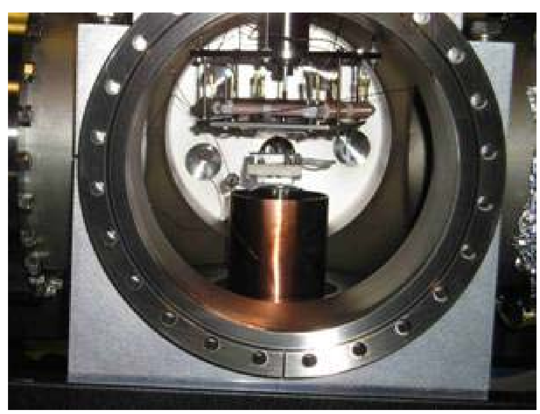

(a) (b)

Fig. 1. The secondary electron emission test stand (a) in construction phase with (b) a close-up view of the electron gun, detector, grid, and cryostat assembly.

Between August of 2004 to January 2005, considerable effort was placed in coordinating the operation of each component of the test stand. Electronic measurements were compared against manufacture's measurements and software output. Limitations of the test stand were also examined. Although the cryostat cold head reaches 8.5 ^{o}K, the sample itself only reaches temperatures of about 15 ^{o}K as measured by a temperature diode attached to the cryohead surface. This is due to the large thermal gradient posed to the sample and the thermal power limitations of the cryohead.

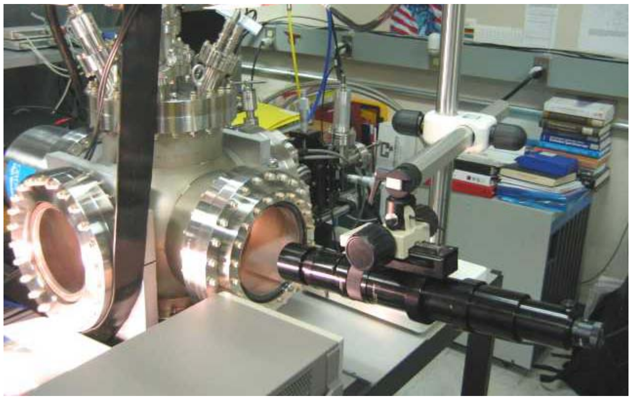

Fig. 2. A long range microscope is used to examine both the electron beam diameter impinging on a phosphorescence screen and the surface structure of the piece under test.

Working within the limitations of the secondary electron emission test stand, sample studies were conducted at room temperature on a non-surfaced cleaned niobium sample. An experimental procedure was developed using the detector as a means to determine which beveled surface lies within the path of the beam. Figure 2 depicts a long range microscope used to measure the electron beam width. The same microscope is used to show the different beveled surfaces and the texture of the surfaces under test as demonstrated in Figure 3. The overall extent of the gauge in the figure measures 0.5 mm. The striations of the sample surface are very noticeable on this sample.

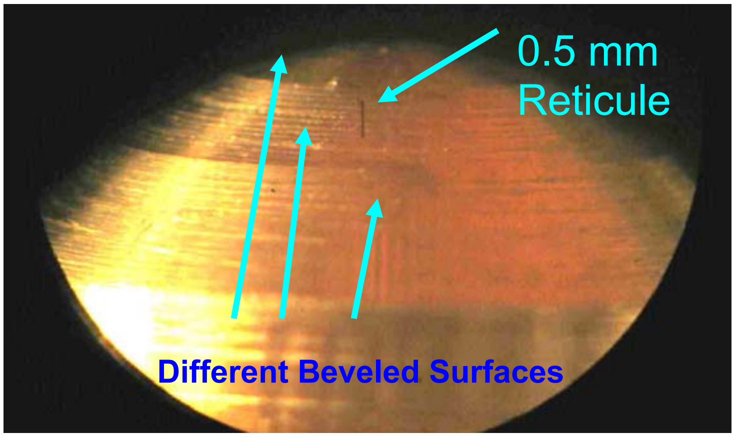

Fig. 3. Machine cut niobium sample prior to surface conditioning as pictured in the SEE test stand. Three beveled surfaces can be seen with machine cut striations over the sample surface. A 0.5 mm reticule is also shown in the figure. All samples prior to cleaning have been machined by the same machine shop in the same manner.

Current experiments have been performed with a 1 keV primary electron beam impinging on a sample surface within a 10 second acquisition time. A 100 V grid potential and a 2.4 kV MCP (micro-channel plate) potential were imposed. The sample to grid distance is 1". Figures 4a and 4b provide typical secondary electron position data that have been conditioned for a primary beam impinging at a 15^{o} angle to the normal of the niobium surface. Both dark noise and count levels less than five have been subtracted from the raw data. Primary beam currents are typically measured with a Faraday Cup. Although not measured for these specific shots, the beam current is on the order of 8 nA based on past measurements. Because of the striations in the unconditioned sample, one would suspect that the a small change in sample position might result in a difference in the secondary electron emission pattern. It is observed in Fig. 4b that the SEE count was about twice that of Fig. 4a. The "sweet spot" of the secondary electron emission noticeably shifted.

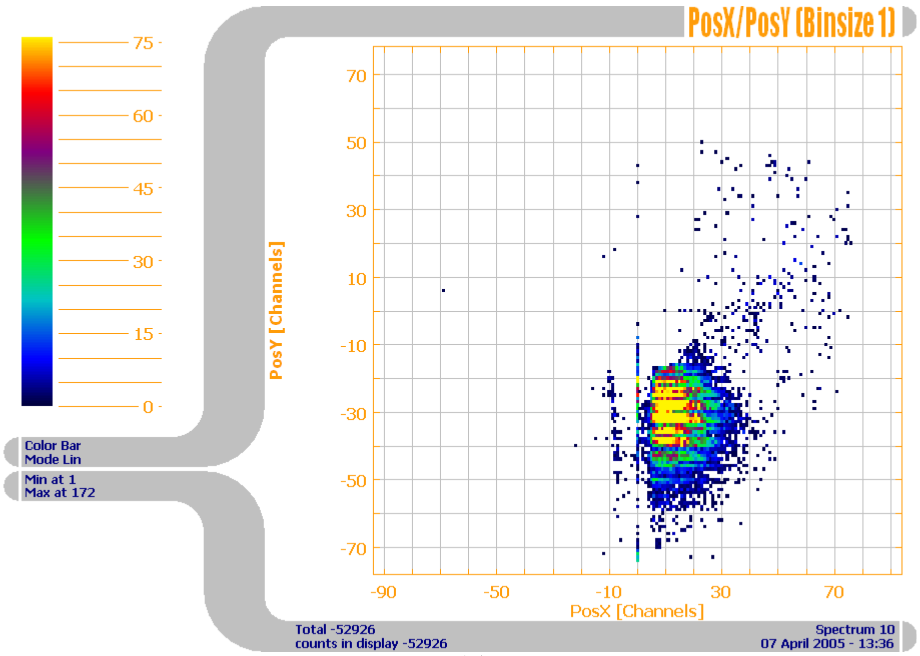

(a)

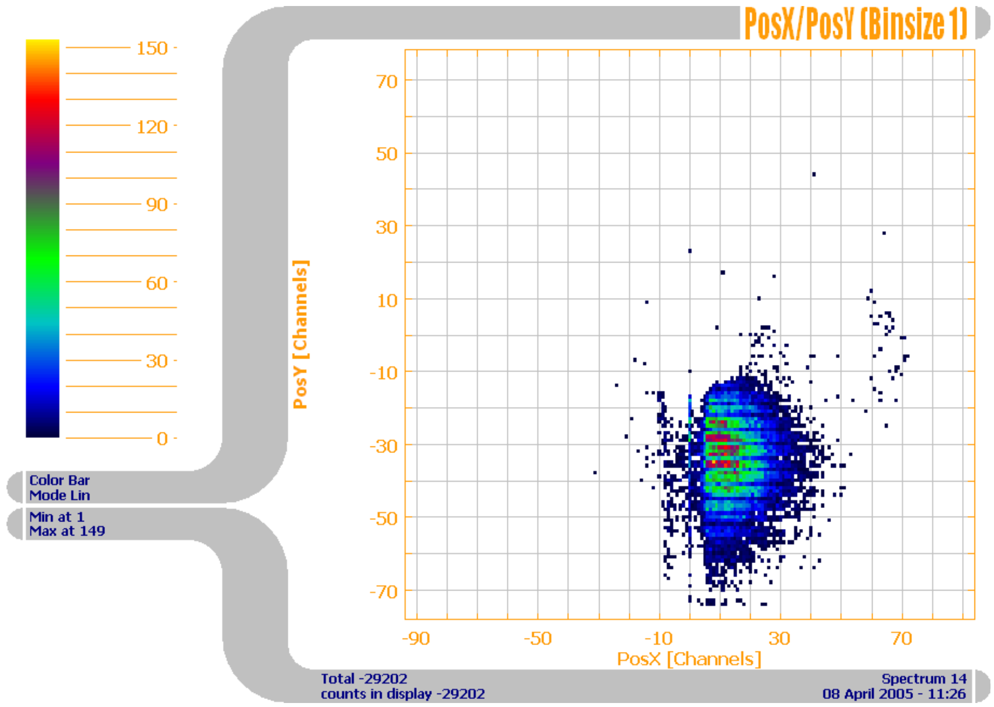

(b)

Fig. 4. Secondary electron emission particle position data due to a 1 keV electron beam impinging 15 ^{o} to the normal of the surface of an untreated, machined, niobium surface. Note that the electron count in (a) is about half of that in (b). The difference in the experimental setup between (a) and (b) is a slight change in sample position. The difference in count may be a consequence of emission at a crest of a striation being released to the vacuum region being different than that at a valley in the striation. In the valley of a striation, some of the secondary electrons could be captured by the striation walls. A noticeable shift in the average location of the highest concentration of secondary electrons on the detector surface is observed between the two locations. The striation places a different angle of surface in the path of the beam.

Based on particle tracking simulations, a family of initial energies and momenta are determined for a point in the "sweet spot" of the data measured. Neglecting the effect of striations, it is assumed that the angle the beam makes with the normal of the surface is equivalent to the angle of the bevel. This assumes that the surface is smooth as should be the case in the conditioned surfaces to be tested in the future. From Fig. 4a, the (10,-30) point was translated to appropriate location on the sample surface. Figure 5 provides all of the possible initial energy and momentum angles that will lead to the final particle position location.

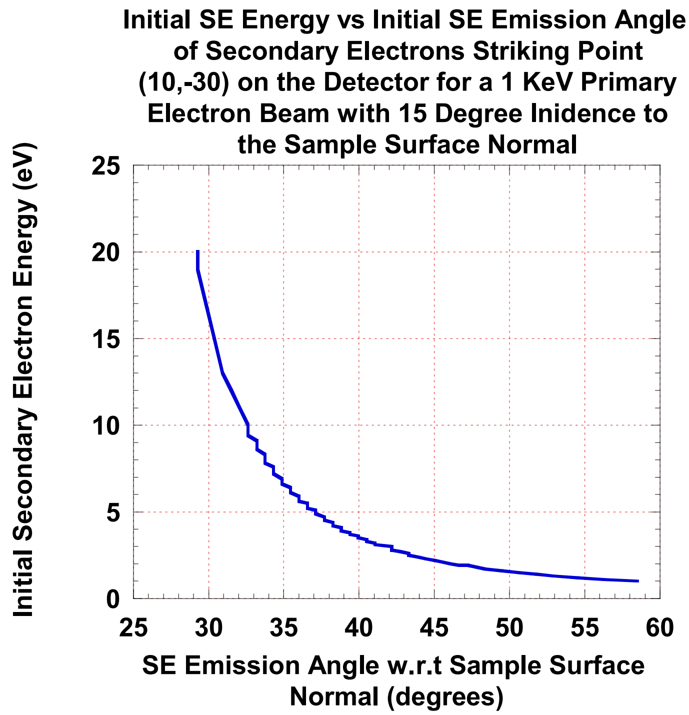

Fig. 5. A family of initial energy and momentum conditions leading to the final condition of a electrons detected in the "sweet spot" of the secondary electron emission. This data is based on the secondary electrons being launched in the central region of the 15^{o} bevel.

In future studies, the results of simulations based on the SEE Monte Carlo code will be compared against experimental results. Accuracy of the model and experiment will be verified.